

Binding of Apo and Glycated Human Serum Albumins to an Albumin-Selective Aptamer-Bound Graphene Quantum Dot Complex

Sirin Sittivanichai, Jitti Niramitranon, Deanpen Japrun^{*} and Prapasiri Pongprayoon^{*}Cite This: *ACS Omega* 2023, 8, 21862–21870

Read Online

ACCESS |



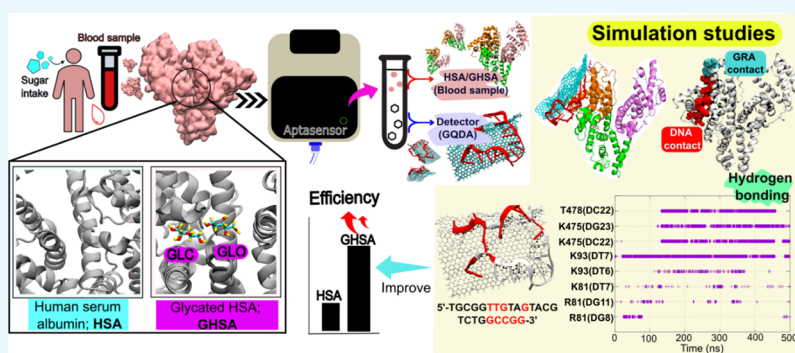
Metrics & More



Article Recommendations



Supporting Information



ABSTRACT: Diabetes mellitus is a chronic metabolic disease involving continued elevated blood glucose levels. It is a leading cause of mortality and reduced life expectancy. Glycated human serum albumin (GHSA) has been reported to be a potential diabetes biomarker. A nanomaterial-based aptasensor is one of the effective techniques to detect GHSA. Graphene quantum dots (GQDs) have been widely used in aptasensors as an aptamer fluorescence quencher due to their high biocompatibility and sensitivity. GHSA-selective fluorescent aptamers are first quenched upon binding to GQDs. The presence of albumin targets results in the release of aptamers to albumin and consequently fluorescence recovery. To date, the molecular details on how GQDs interact with GHSA-selective aptamers and albumin remain limited, especially the interactions of an aptamer-bound GQD (GQDA) with an albumin. Thus, in this work, molecular dynamics simulations were used to reveal the binding mechanism of human serum albumin (HSA) and GHSA to GQDA. The results show the rapid and spontaneous assembly of albumin and GQDA. Multiple sites of albumins can accommodate both aptamers and GQDs. This suggests that the saturation of aptamers on GQDs is required for accurate albumin detection. Guanine and thymine are keys for albumin-aptamer clustering. GHSA gets denatured more than HSA. The presence of bound GQDA on GHSA widens the entrance of drug site I, resulting in the release of open-chain glucose. The insight obtained here will serve as a base for accurate GQD-based aptasensor design and development.

INTRODUCTION

Diabetes mellitus is a chronic metabolic disease involving continued elevated blood glucose levels. Severe diabetes can cause serious complications such as blindness, kidney failure, heart attacks, and cerebral infarction.^{1–3} Monitoring fasting blood glucose and glycated hemoglobin (HbA1c) is a common measure for diabetes screening and diagnosis.⁴ Thus, many HbA1c-detecting strategies have been designed for effective HbA1c detection.^{5–7} However, such methods are not suitable for pregnant women and patients with kidney and/or cardiovascular diseases.^{8,9} Thus, new effective biomarkers for diabetes screening and monitoring are in urgent need. To date, glycated human serum albumin (GHSA) has been suggested as a new promising diabetes biomarker.^{10–14} In diabetes patients, the GHSA level can be 2–3-fold higher than that of healthy people.^{15,16} No fasting is required for GHSA measurement.

GHSA was reported to provide more relevant and immediate glucose information relative to HbA1c in children, adolescents, and pregnant women.^{17,18} Therefore, many attempts have been made to search for GHSA detection strategies.^{19–21} Previously, liquid chromatography,^{22,23} affinity chromatography,^{24,25} colorimetry,²⁶ Raman spectroscopy,²⁷ and immunochemistry²⁸ were studied to detect a GHSA level; however, such methods are costly and time-consuming. More convenient and faster techniques such as a lateral flow assay,¹⁷ an electrochemical

Received: March 9, 2023

Accepted: May 23, 2023

Published: June 6, 2023



immunoassay,²⁹ specific gel electrophoresis,³⁰ and optical biosensors^{20,31–35} are introduced.

One of the promising techniques is nanomaterial-based aptasensors due to their good selectivity and sensitivity and cost-effectiveness.^{36–38} For nanomaterial-based aptasensors, a short DNA aptamer was employed as a recognition molecule to detect an analyte such as GHSA. Nanomaterials such as metal nanoparticles,³⁹ graphene,^{33–40} and graphene quantum dots (GQDs)⁴¹ were used as a substrate and/or a luminophore. Among nanomaterials, zero-dimensional nanosized GQDs have come into focus because of their unique photoluminescence properties, high photostability, non-toxicity, and especially more biocompatibility when compared to other nanosized materials.^{42–45} The capability to be a good substrate for biomolecules and quenching agents⁴⁶ also allows the involvement of GQDs in many disease biosensor platforms, including GHSA detection.^{40,41,47–50} GQDs were used in aptasensors as an aptamer linker and/or a fluorescence quencher.^{20,31,32,51} For fluorescent aptasensors, analyte-selective fluorescent aptamers are first adsorbed onto GQDs in a solution, resulting in fluorescence quenching. The presence of analytes such as albumin induces the release of an aptamer to a target, resulting in fluorescence recovery. Several studies indicate the high sensitivity of GQD-based aptasensors,^{41,52,53} but the molecular insight into the formation of GQD-aptamer-GHSA complexes in GQD-based aptasensors is still limited. Especially, how albumin recognizes and interacts with a GQD-bound aptamer in an aqueous solution remains unclear. Such information is important for accurate design and development of potential GQD-based aptasensors. Therefore, in this work, the recognition mechanism of albumin to a GQD-bound DNA aptamer in an aqueous solution is revealed. Both GHSA and human serum albumin (HSA) are studied in comparison.

HSA has a heart-like shape composed of 585 amino acids with three homologous domains (I, II, and III). Each domain contains two subdomains (A and B) (Figure 1A). HSA has two drug sites [Sudlow sites I (warfarin–azapropazone binding site) and II (indole–benzodiazepine binding site)] located inside domains IIA and IIIA (Figure 1A). In the presence of blood glucose, a free amino group on HSA interacts with an aldehyde group on glucose to form an Amadori product.^{54–56} Recently, a crystal structure of GHSA has been solved.⁵⁷ Two glucose molecules [open- (GLO) and closed- (GLC) forms] were found inside drug site I or Sudlow site I (Figure 1A). A previous work shows that the GHSA structure gets damaged more than HSA during binding to a bare GQD.⁵⁰ This may interfere with the binding ability of albumin to an aptamer probe in an aptasensor. To better understand the formation of a GHSA-aptamer-GQD complex in a solution, molecular dynamics (MD) simulations were performed here. The assemblies of HSA and GHSA to the GQD-aptamer complex (GQDA) are studied in comparison. Two different albumin orientations (front and back poses facing GQDA) are investigated to mimic possible binding poses of albumin onto the aptamer-GQD complex (Figure 1C). Both front and back orientations used here are based on previously reported ligand-binding sites on an albumin surface.^{52–62} The insight obtained here will serve as a base for accurate GQD-based aptasensor design and development.

MATERIALS AND METHODS

The 10 ns equilibrated structures of both GHSA and HSA were obtained from previous studies,^{63,64} where their initial

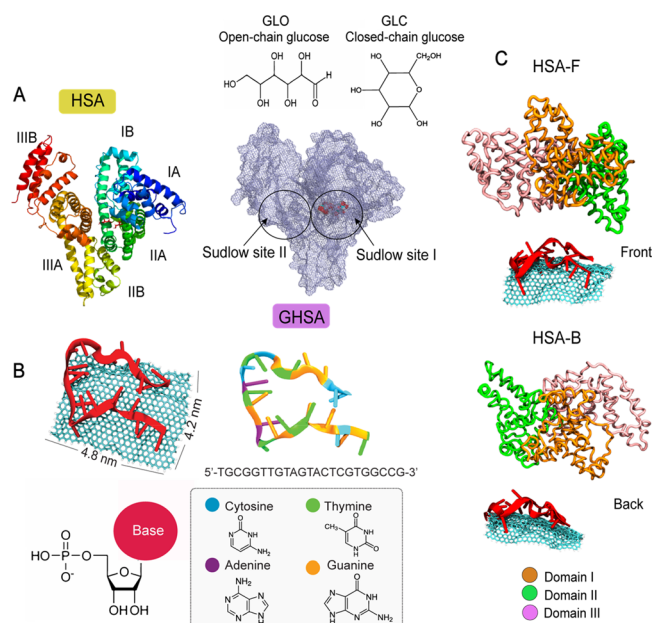


Figure 1. (A) Cartoon representations of apo HSA (left) and GHSA (right) where two glucose molecules are located at Sudlow site I. The albumin-selective DNA aptamer in a complex with a GQD is shown in (B). Two initial conformations of albumin (front and back) on an aptamer-GQD complex in this work are shown in (C).

structures were adopted from the Protein Data Bank (PDB codes: 1E78 and 4IW2). The GHSA-selective aptamer sequence was obtained from a previous work.³³ This aptamer shows high selectivity for GHSA than other abundant proteins such as IgG and Hb in blood.⁵² This single-stranded DNA aptamer contains 23 nucleotides comprising 5'-TGCGGTTGTAGTACTCGTGGCCG-3' (Figure 1C). A GQD sheet has a dimension of 48 Å × 42 Å constructed by a Nanotube Builder module implemented in the Visual Molecular Dynamics (VMD) program.⁶⁵ A GQD topology was generated using OPLS forcefields.⁶⁶ The GQD-aptamer complex (GQDA) was taken from a previous study,⁶⁷ where the GQD-aptamer complex used here was obtained from the 200 ns final snapshot of a GQD-aptamer assembly. For each albumin, two systems where a GQD-aptamer was placed at a distance of 10 Å from the back (B) and front (F) of a protein were set (see Figure 1C for initial configurations). The infixes of “-F” and “-B” refer to the GQDA position. Two repeats were performed for each albumin. The suffixes of “_1” and “_2” were used for repeats (1 and 2). Four simulations were performed for HSA (HSA-F1, HSA-F2, HSA-B1, and HSA-B2) and GHSA (GHSA-F1, GHSA-F2, GHSA-B1, and GHSA-B2). There are eight systems in total. For each system, the complex was placed in an 11 × 11 × 11 nm³ periodic cubic box. Each system was neutralized by counter ions and solvated with TIP3P water molecules⁶⁸ and 1 M NaCl.

MD simulations were conducted using GROMACS 2020 packages (www.gromacs.com) with Amber ff99SB-ILDN.⁶⁹ The energy minimization was done for 5000 steps using steepest descent algorithms to relax steric conflicts generated during the setup. Long-range electrostatic interactions were treated using the particle mesh Ewald method⁷⁰ with a short-range cutoff of 1 nm, a Fourier spacing of 0.12 nm, and fourth-order spline interpolation. All simulations were performed in a constant number of particles, pressure, and temperature

(NPT) ensemble. All bonds were constrained by LINCS algorithms.⁷¹ The temperatures of the protein, solvent, and ions were each coupled separately using the v-rescale thermostat⁷² at 300 K with a coupling constant $\tau_t = 0.1$ ps. The pressure was coupled using the Berendsen algorithm at 1 bar with a coupling constant $\tau_p = 1$ ps. The time step for integration was 2 fs. Coordinates were saved every 2 ps for subsequent analysis. The 10 ns equilibration runs were performed and followed by the 500 ns production runs.

All results provided here are the average values from two repeats. The data were analyzed by GROMACS and locally written code. Hydrogen bonds were computed using the “gmhbond” option where the hydrogen-donor-acceptor cutoff angle was set to 30° and the cutoff radius (X-acceptor) was 0.35 nm. “Gmhbond” was also used to compute the number of contacts using the “-contact” option. Molecular graphic images were prepared using VMD.⁶⁵ C-alpha RMSD and RMSF calculations were computed using an initial structure from each production run as a reference. Secondary structure analysis was calculated by “do_dssp” command.

RESULTS AND DISCUSSION

At the beginning, the decreased albumin-GQDA distances in Figure 2A,B clearly demonstrate the fast and spontaneous adsorption of the GQD-aptamer complex onto both albumins. The front and back sides of albumin can adhere on GQDA. However, HSA and GHSA seem to induce the difference in GQDA binding abilities. The diverse HSA-GQDA distances in

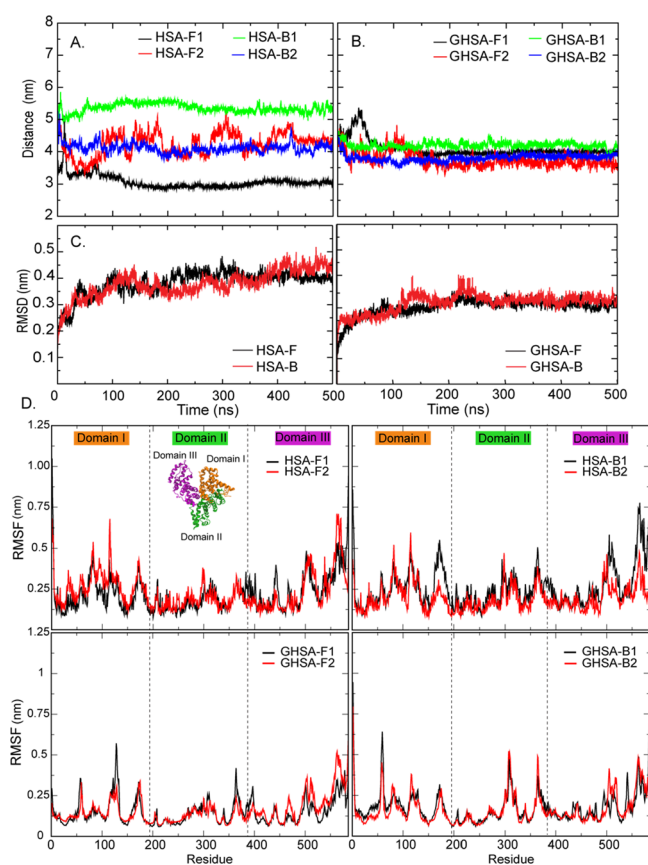


Figure 2. (A) and (B) Distances between the centers of masses of albumin and GQDA in all systems. (C) Average C-alpha RMSDs of albumins in all systems. (D) Protein RMSFs of all systems.

Figure 2A imply the various HSA-GQDA packing abilities, while both the front and back sides of GHSA can fasten GQDA with a similar degree of compactness (the constant GHSA-GQDA distances of ~ 0.4 nm in Figure 2B). This difference may be due to the GHSA-selective DNA aptamer used in this work.^{33,73} In addition, the structural drift and fluctuation of HSA and GHSA are measured via the root-mean-square deviations (RMSDs) and root-mean-square fluctuations (RMSFs) of all C-alpha atoms (Figure 2C,D). RMSDs of all systems are shown in Figure S1 in the Supplementary Information. Overall, HSA shows slightly higher structural flexibility than GHSA in both front and back binding poses (Figure 2C). Domains I and III seem to show high flexibility, especially domain I (Figure 2D). Such higher structural flexibility is driven by the high mobility of subdomain IA in all cases (Figure 3). Not only subdomain IA

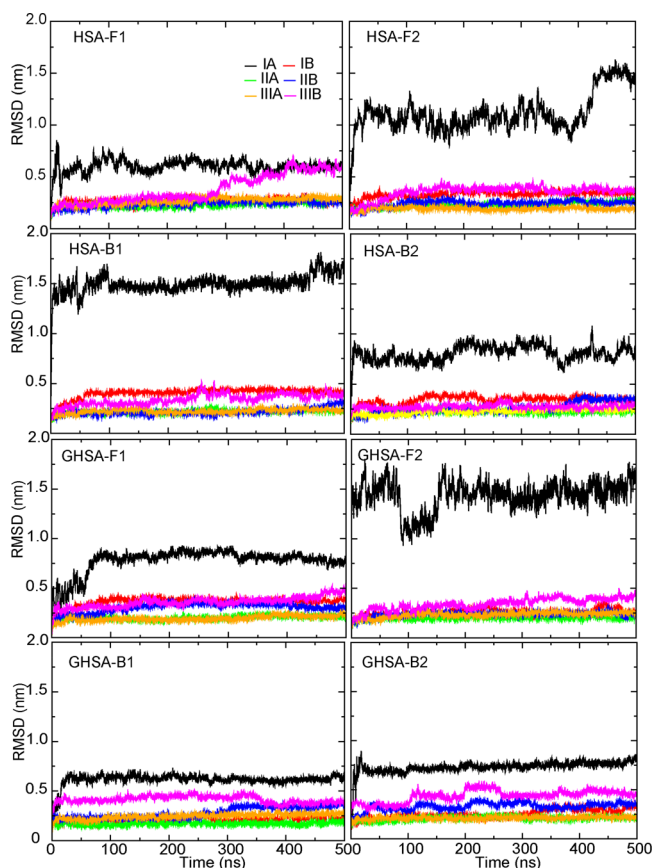


Figure 3. C-alpha RMSDs of each subdomain in HSA and GHSA systems. Subdomains IA, IB, IIA, IIB, IIIA, and IIIB are colored in black, red, green, blue, orange, and magenta, respectively.

but subdomain IIIIB is also found to contribute to the structural fluctuation (Figure 3). Like HSA, subdomain IA of GHSA is also mobile. Compared to apo albumins,^{63,64,73,74} domain III was reported to be mobile in a solution, whereas the presence of bound GQDA here significantly reduces the dynamics of domain III and concurrently enhances the mobility of subdomain IA (Figure 3). The presence of bound GQDA seems to induce a significant change in the structural dynamics of albumins.

To further investigate the change in the protein structure, the secondary structures of all albumins are computed and compared to apo HSA and free GHSA in Table 1. The binding

Table 1. Secondary Structure of Albumins in All Cases Compared to Bare HSA and GHSA

system	secondary structure percentage (%)		
	helix (%)	loops and turns (%)	coil (%)
free HSA	65.82	20.85	14.36
HSA-F1	55.56	24.79	14.02
HSA-F2	59.18	23.51	12.83
HSA-B1	58.12	24.44	12.31
HSA-B2	59.83	23.42	12.99
free GHSA	70.26	16.41	11.79
GHSA-F1	57.26	24.79	12.82
GHSA-F2	57.43	23.42	12.99
GHSA-B1	57.95	24.62	13.85
GHSA-B2	58.27	22.74	14.53

of GQDA to an albumin seems to destroy the helical structure significantly (Table 1). The apo HSA and free GHSA can maintain ~65–70% helicity, but the binding of GQDA causes ~5–15% helical denaturation (Table 1). The more GQDA contacts are formed, the more protein structures are denatured. Especially, the glucose-bound GHSA (~12–13%) appears to be denatured more than HSA (~5–10%). This may be due to the presence of bound glucose. More details will be discussed later in the text.

In terms of GQDA binding, the multiple GQDA binding sites on an albumin are captured (Figure 4A,B). However, such areas are the same DNA-binding sites as reported in a previous work of a free albumin in a solution.⁷³ An albumin in GHSA-F1 induces the highest number of GQDA contacts (~286 contacts) due to the interactions with a bare GQD surface (Figure 4B). Seemingly, domain II contributes to all HSA-GQDA complex formation with different degrees of binding

ability, while domains I and III are the main player for the tight binding in most cases (Table 2). Exceptionally, GHSA-F2 employs domain II for the attachment, while GHSA-B1 and GHSA-B2 require both domains I and II (Table 2 and Figure 4A,B). For GQDA, both DNA and GQD contribute to the albumin-GQDA assembly with different degrees of binding ability (Figure 4C). It is interesting that only DNA is adequate to induce the albumin-GQDA assembly in HSA-F1 (Figure 4C). However, GQD is also able to interact with an albumin, as seen in GHSA-F1 (Figure 4C), which is commonly found in previous studies.^{50,75,76} The favorable binding energies can also confirm that both an aptamer and GQD can attract albumins, but an aptamer is more attractive for albumins (Table S2 in the Supplementary Information). However, the ability of GQDs to bind to albumins highlights the requirement of full GQD coverage for a precise aptamer-GQD-based albumin detection. A set of albumin-DNA hydrogen bonds are also computed in Figure 4D. The number of albumin-DNA hydrogen bonds is maximized when a DNA aptamer binds to the back of domain III (~17–28 hydrogen bonds in GHSA-B1 and GHSA-B2), while the binding to the albumin center requires ~8 hydrogen bonds to stabilize the complex (Figure 4D). It can be seen from Figure 4C,D that the association of albumin and GQDA employs both electrostatic (hydrogen bonds) and hydrophobic forces. The influence of such interactions depends on the binding position on GQDA. Seemingly, DNA attracts an albumin by electrostatic interactions, whereas GQD uses hydrophobic forces to drive the GQDA-albumin clustering. For example, HSA-F2, HSA-B1, HSA-B2, and GHSA-F1 form a low number of albumin-DNA hydrogen bonds due to the presence of more GQD contacts (Figure 4C). In contrast, when an albumin is adhered by DNA, a high number of hydrogen bonds are captured (Figure 4D). This finding

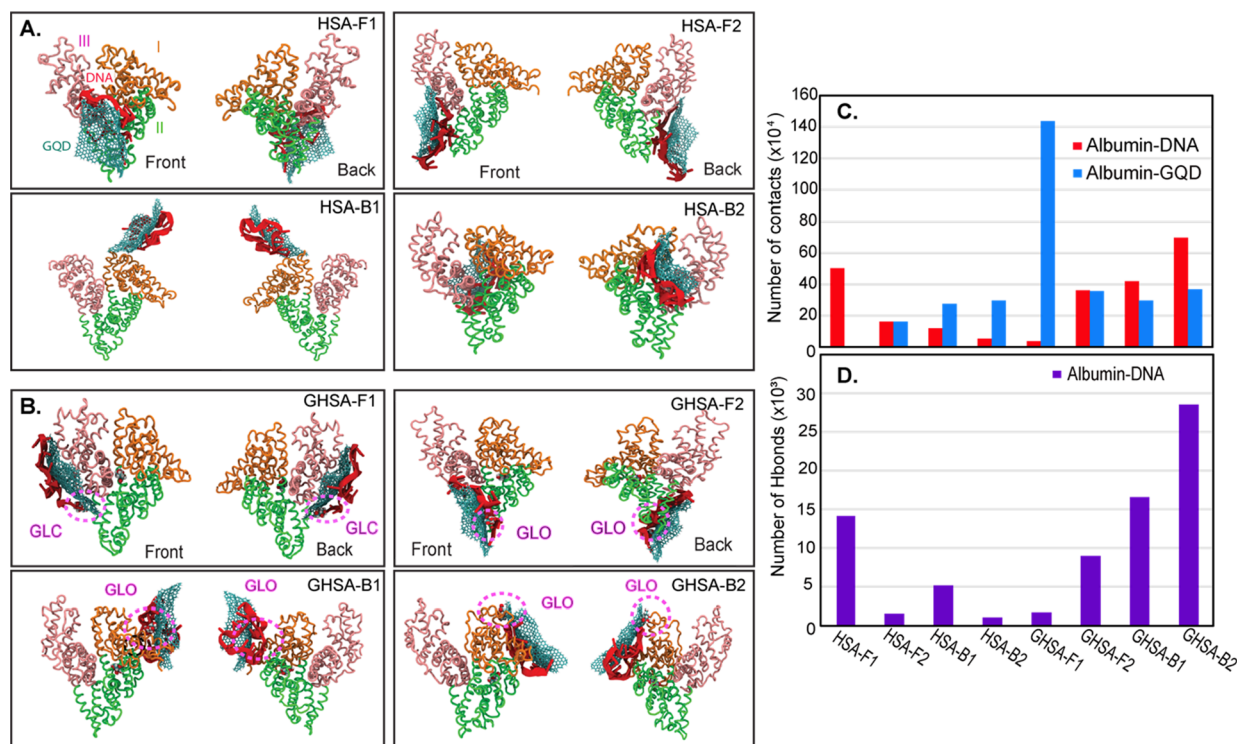


Figure 4. Final snapshots of HSA (A) and GHSA (B) systems. A number of albumin-DNA and albumin-GQD contacts are shown in (C). Hydrogen bonds between albumin and DNA are displayed in (D).

Table 2. Average Number of Contacts with Standard Deviation between Each Domain and GQDA Complex^a

system	domain I (1–192)	domain II (193–385)	domain III (386–585)
HSA-F1	78.97 ± 30.72	2.58 ± 5.72	107.45 ± 53.45
HSA-F2	4.09 ± 13.57	42.94 ± 15.36	110.42 ± 27.43
HSA-B1	157.81 ± 44.26	1.37 ± 5.47	0
HSA-B2	49.92 ± 20.06	2.07 ± 6.57	88.25 ± 19.00
GHSA-F1	0	24.96 ± 33.14	262.04 ± 99.05
GHSA-F2	0	112.40 ± 24.44	31.28 ± 18.91
GHSA-B1	65.94 ± 19.27	78.75 ± 14.88	0
GHSA-B2	104.33 ± 30.41	103.01 ± 24.10	0

^aOnly contacts within 0.35 nm are counted here.

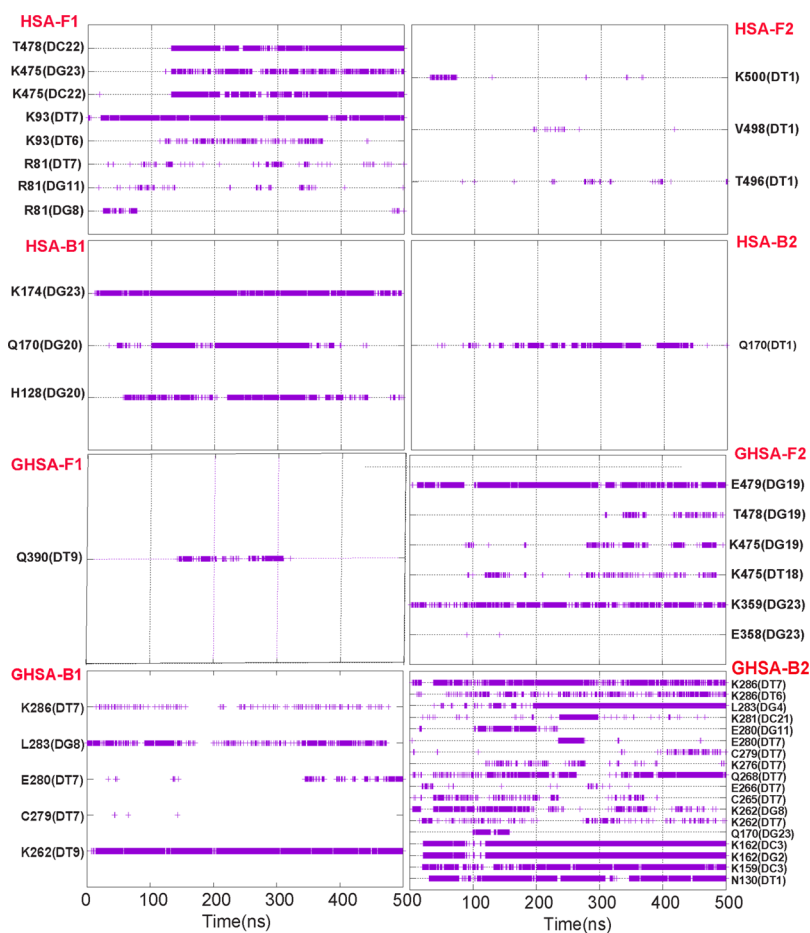


Figure 5. Occurrence of hydrogen bonds as a function of time in all systems.

demonstrates the ability of both hydrophobic and electrostatic interactions for GQDA-albumin clustering. However, except GHSA-F1, it is noticeable that most GHSAs seem to produce more DNA contacts than HSA (Figure 4C). This may be due to more GHSA-selective aptamers as reported in a previous work.⁷³

To explore how DNA interacts with an albumin, the hydrogen bonds between an albumin and aptamer are computed in Figure 5. Positively charged residues, lysine and arginine, are found to play a dominant role in albumin-DNA adhesion (Figure 5). This is due to the attraction from a phosphate backbone on DNA (Table S1 in the Supplementary Information). Nonetheless, other polar and apolar residues (such as glutamic acid, leucine, valine, cysteine, glutamine, and threonine) also contribute to such DNA-albumin clustering (Figure 5). Nucleobases can also interact with both albumins

(Table S1 in the Supplementary Information). Seemingly, an albumin can bind to most of the DNA chain, except residues 12–17. Such an area is located close to the top of the hairpin region and aligned on the edge of the GQD (Figures S2 and S3 in the Supplementary Information). Guanine (G) and thymine (T) seem to be preferable for binding to albumin (Figure 5). In the case of HSA-F1 and GHSA-B2, where a high number of DNA interactions are captured, both albumins mostly interact with two legs of an aptamer (residues 1–11 and residues 19–23) (Figures 6 and S3 in the Supplementary Information). Compared to a GQD-free system from a previous work,⁷³ both 3' and 5' ends of DNA were found to play a role in DNA-albumin adduct formation. This suggests that the aptamer contains an albumin-specific region. In contrast, HSA-F2, HSA-B2, and GHSA-F1 can generate a few number of hydrogen bonds with DNA owing to the large exposure to

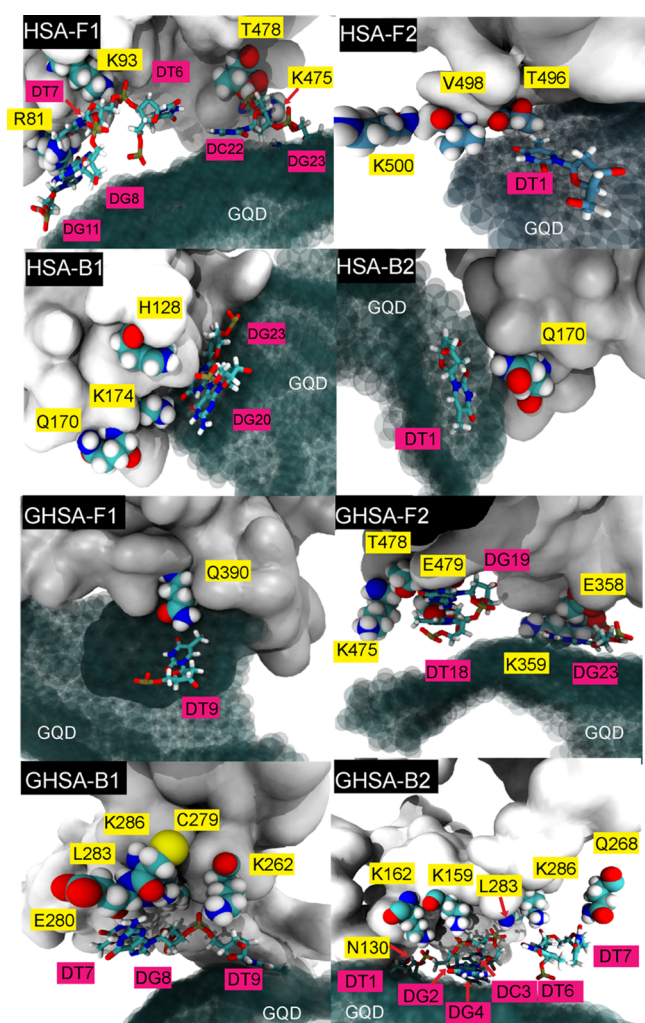


Figure 6. Cartoon views of key residues involved in the albumin-GQDA hydrogen bonding network. Yellow labels indicate key amino acids, whereas pink bands show key nucleobases.

the GQD surface (Figures 4C, 5, and 6). The locations of key residues involved in the interaction network are displayed in Figure 6.

In addition, the effect of GQDA-albumin clustering on two glucose molecules inside GHSA is also investigated. The exit of bound glucose is found. This is due to the slight widening of the entrance of drug site I measured by distances between pairs of G202-V455 and R218-D451 located at the entrance (Table S3 in the Supplementary Information). Ligand-free albumins (HSA) seem to maintain their drug site I's volumes, while the clear expansion of the mouth of drug site I is captured in

glucose-bound systems (GHSA) (Table S3 in the Supplementary Information). For the GHSA system, due to the wider entrance, open-chain glucoses (GLOs) mostly escape out of a drug site, except GHSA-F1 where all sugar molecules are released (Figure 4). In the case of GHSA-F1, GLC is adsorbed on GQDA and GLO binds to the HSA surface. Unlike GHSA-F1, GLCs in other systems are kept inside a pocket because it is more buried; however, GLC remains water-accessible (Table 3). The more water exposure of GLO and its location close to the wide pocket entrance seem to facilitate its escape. When GLO is released to the bulk, it binds to the GQDA complex where more GQD-GLO contacts are captured (Table 3). Nonetheless, such escaping GLOs can hydrogen bond with an aptamer (Figure S4 and Table S4 in the Supplementary Information). The release of glucoses observed here also illustrates that the binding of GQDA significantly interferes with the accessibility of drug site I.

CONCLUSIONS

In this work, the mechanism of albumin-GQDA adduct formation is investigated to better understand the underlying mechanism of GQD-based aptasensors for albumin detection. The result shows that the aggregation of albumin and GQDA is rapid and spontaneous. Multiple binding sites for GQDA on albumin are identified. The top of the hairpin region of an aptamer at the edge of the GQD seems to be the least favorite site for albumin binding. Guanine (G) and thymine (T) seem to be the major target for albumin attack. GHSA seems to be more preferable to the GQDA complex than HSA. Albumin can interact with both GQD and DNA, confirming the requirement of full coverage of the GQD surface from a previous work⁵⁰ to prevent misleading data. Herein, no desorption of an aptamer is revealed. More adhered aptamers are needed to enhance the chance of DNA desorption. In addition, the binding of the GQDA complex also seriously destroys the glucose-binding ability of GHSA by widening the drug site entrance. The formation of the GHSA-GQDA adduct appears to significantly impact the ligand-binding ability of drug site I. The desorption behavior of albumin-DNA-GRA to mimic the step of fluorescent recovery in an aptasensor will be our further study to comprehend the activity of the aptasensor in detail.

ASSOCIATED CONTENT

Supporting Information

The Supporting Information is available free of charge at <https://pubs.acs.org/doi/10.1021/acsomega.3c01595>.

C-alpha RMSDs of HSA and GHSA; aptamer-GRA complex; cartoon views of GQDA and albumin with residues from GQDA and albumins involved in the

Table 3. Number of Contacts of Each Sugar with Albumin, DNA, GQD, and Water

system	sugar	albumin	DNA	GQD	water
GHSA-F1	GLC	0.25 ± 0.04	16.31 ± 9.08	31.04 ± 8.23	127.82 ± 18.49
	GLO	116.20 ± 13.72	0	0	74.57 ± 14.38
GHSA-F2	GLC	125.35 ± 17.87	0	0	53.21 ± 17.20
	GLO	0.15 ± 0.06	21.78 ± 10.31	28.69 ± 7.44	123.07 ± 20.02
GHSA-B1	GLC	95.53 ± 14.04	0	0	81.93 ± 22.46
	GLO	46.63 ± 11.49	19.88 ± 5.55	31.49 ± 7.58	84.37 ± 17.58
GHSA-B2	GLC	103.45 ± 13.46	0	0	51.18 ± 13.59
	GLO	22.37 ± 12.69	7.06 ± 8.88	25.73 ± 7.86	108.91 ± 20.35

albumin-GQDA assembly; final snapshots of GQDA complexes from all systems; number of hydrogen bonds between albumin and aptamer components; and interaction energies of albumin (Prot) with the aptamer (DNA) and GQD (PDF)

AUTHOR INFORMATION

Corresponding Authors

Deanpen Japrun – National Science and Technology Development Agency, National Nanotechnology Center, Pathumthani 12120, Thailand; Phone: +66-2564-6665; Email: deanpen@nanotec.or.th; Fax: +66-2564-6985

Prapasiri Pongprayoon – Department of Chemistry, Faculty of Science, Kasetsart University, Bangkok 10900, Thailand; Center for Advanced Studies in Nanotechnology for Chemical, Food and Agricultural Industries, KU Institute for Advanced Studies, Kasetsart University, Bangkok 10900, Thailand; orcid.org/0000-0002-1472-8241; Phone: +66-2562-5555; Email: fsciprpo@ku.ac.th; Fax: +66-2579-3955

Authors

Sirin Sittivanichai – Department of Chemistry, Faculty of Science, Kasetsart University, Bangkok 10900, Thailand

Jitti Niramitranon – Department of Computer Engineering, Kasetsart University, Bangkok 10900, Thailand

Complete contact information is available at:
<https://pubs.acs.org/10.1021/acsomega.3c01595>

Notes

The authors declare no competing financial interest.

ACKNOWLEDGMENTS

We would like to thank Kasetsart University Research and Development Institute (Grant no. FF(KU)25.64), National Nanotechnology Center, National Science and Technology Development Agency (Grant no. P2251069), the Office of the National Economic and Social Development Council, and the Office of the Prime Minister through Kasetsart University under the project entitled “Driving Research and Development of Cutting-edge Innovations for ASEAN’s Agricultural Leadership” for financial support. This work was also supported by the Royal Golden Jubilee (RGJ) Ph.D. Program (PHD/0131/2561). We also thank NSTDA Supercomputer Center (ThaiSC) for computer facilities.

ABBREVIATIONS

HSA human serum albumin
GHSA glycated human serum albumin
GLC closed-chain glucose
GLO open-chain glucose
GQD graphene quantum dot
GQDA graphene quantum dot-aptamer complex

REFERENCES

- (1) Folsom, A. R.; Ma, J.; Eckfeldt, J. H.; Nieto, F. J.; Metcalf, P. A.; Barnes, R. W. Low serum albumin. Association with diabetes mellitus and other cardiovascular risk factors but not with prevalent cardiovascular disease or carotid artery intima-media thickness. The Atherosclerosis Risk in Communities (aric) study investigators. *Ann. Epidemiol.* **1995**, *5*, 186–191.
- (2) Tripathi, B. K.; Srivastava, A. K. Diabetes mellitus: complications and therapeutics. *Med. Sci. Monit.* **2006**, *12*, Ra130–Ra147.
- (3) Rask-Madsen, C.; King, G. L. Vascular complications of diabetes: mechanisms of injury and protective factors. *Cell Metab.* **2013**, *17*, 20–33.
- (4) Feng, X.; Yang, Y.; Zhuang, S.; Fang, Y.; Dai, Y.; Fu, Y.; Hu, Q.; Yuan, Q.; Tang, H.; Tang, L. Influence of serum albumin on HbA1c and HbA1c-defined glycemic status: A retrospective study. *Front. Med. (Lausanne)* **2021**, *8*, No. 583093.
- (5) Mahobiya, S. K.; Balayan, S.; Chauhan, N.; Khanuja, M.; Kuchhal, N. K.; Islam, S. S.; Jain, U. Tungsten disulfide decorated screen-printed electrodes for sensing of glycated hemoglobin. *ACS Omega* **2022**, *7*, 34676–34684.
- (6) Anand, A.; Chen, C.-Y.; Chen, T.-H.; Liu, Y.-C.; Sheu, S.-Y.; Chen, Y.-T. Detecting glycated hemoglobin in human blood samples using a transistor-based nanoelectronic aptasensor. *Nano Today* **2021**, *41*, No. 101294.
- (7) Yazdanpanah, S.; Rabiee, M.; Tahriri, M.; Abdolrahim, M.; Tayebi, L. Glycated hemoglobin-detection methods based on electrochemical biosensors. *Trends Analyt. Chem.* **2015**, *72*, 53–67.
- (8) Bloomgarden, Z.; Handelsman, Y. How does CKD affect HbA1c? *J. Diabetes* **2018**, *10*, 270.
- (9) Tanemoto, M. The analysis of hemoglobin A1c in dialysis patients should include the variables that reflect the erythrocyte turnover. *Kidney Int.* **2018**, *94*, 220–221.
- (10) Beck, R.; Steffes, M.; Xing, D.; Ruedy, K.; Mauras, N.; Wilson, D. M.; Kollman, C.; the Diabetes Research in Children Network (DirecNet) Study Group. The interrelationships of glycemic control measures: HbA1c, glycated albumin, fructosamine, 1, 5-anhydroglucitol, and continuous glucose monitoring. *Pediatr. Diabetes* **2011**, *12*, 690–695.
- (11) Yoshiuchi, K.; Matsuhisa, M.; Katakami, N.; Nakatani, Y.; Sakamoto, K.; Matsuoka, T.; Umayahara, Y.; Kosugi, K.; Kaneto, H.; Yamasaki, Y. Glycated albumin is a better indicator for glucose excursion than glycated hemoglobin in type 1 and type 2 diabetes. *Endocr. J.* **2008**, *55*, 503–507.
- (12) Wu, W. C.; Ma, W. Y.; Wei, J. N.; Yu, T. Y.; Lin, M. S.; Shih, S. R.; Hua, C. H.; Liao, Y. J.; Chuang, L. M.; Li, H. Y. Serum glycated albumin to guide the diagnosis of diabetes mellitus. *PLoS One* **2016**, *11*, No. e0146780.
- (13) Xiong, J.-Y.; Wang, J.-M.; Zhao, X.-L.; Yang, C.; Jiang, X.-S.; Chen, Y.-M.; Chen, C.-Q.; Li, Z.-Y. Glycated albumin as a biomarker for diagnosis of diabetes mellitus: A systematic review and meta-analysis. *World J. Clin. Cases* **2021**, *9*, 9520.
- (14) Bai, Y.; Fang, Y.; Ming, J.; Wei, H.; Zhang, P.; Yan, J.; Du, Y.; Li, Q.; Yu, X.; Guo, M. Serum glycated albumin as good biomarker for predicting type 2 diabetes: a retrospective cohort study of China national diabetes and metabolic disorders survey. *Diabetes Metab. Res. Rev.* **2022**, *38*, No. e3477.
- (15) Fanali, G.; di Masi, A.; Trezza, V.; Marino, M.; Fasano, M.; Ascenzi, P. Human serum albumin: from bench to bedside. *Mol. Aspects Med.* **2012**, *33*, 209–290.
- (16) Bai, X.; Wang, Z.; Huang, C.; Wang, Z.; Chi, L. Investigation of non-enzymatic glycosylation of human serum albumin using ion trap-time of flight mass spectrometry. *Molecules* **2012**, *17*, 8782–8794.
- (17) Ki, H.; Jang, H.; Oh, J.; Han, G.-R.; Lee, H.; Kim, S.; Kim, M.-G. Simultaneous detection of serum glucose and glycated albumin on a paper-based sensor for acute hyperglycemia and diabetes mellitus. *Anal. Chem.* **2020**, *92*, 11530–11534.
- (18) Rodrigo, N.; Glastras, S. The emerging role of biomarkers in the diagnosis of gestational diabetes mellitus. *J. Clin. Med.* **2018**, *7*, 120.
- (19) Inoue, Y.; Inoue, M.; Saito, M.; Yoshikawa, H.; Tamiya, E. Sensitive detection of glycated albumin in human serum albumin using electrochemiluminescence. *Anal. Chem.* **2017**, *89*, S909–S915.
- (20) Putnin, T.; Waiwinya, W.; Pimalai, D.; Chawjiraphan, W.; Sathirapongsasuti, N.; Japrun, D. Dual sensitive and rapid detection of glycated human serum albumin using a versatile lead/graphene nanocomposite probe as a fluorescence–electrochemical aptasensor. *Analyst* **2021**, *146*, 4357–4364.

- (21) Iles, R. K.; Iles, J. K.; Lacey, J.; Gardiner, A.; Zmuidinaite, R. Direct detection of glycated human serum albumin and hyperglycosylated IgG3 in serum, by MALDI-ToF mass spectrometry, as a Predictor of COVID-19 severity. *Diagnosics (Basel)* **2022**, *12*, 2521.
- (22) Day, J. F.; Thorpe, S. R.; Baynes, J. W. Nonenzymatically glycosylated albumin. In vitro preparation and isolation from normal human serum. *J. Biol. Chem.* **1979**, *254*, 595–597.
- (23) Guthrow, C. E.; Morris, M. A.; Day, J. F.; Thorpe, S. R.; Baynes, J. W. Enhanced nonenzymatic glycosylation of human serum albumin in diabetes mellitus. *Proc. Natl. Acad. Sci. U. S. A.* **1979**, *76*, 4258–4261.
- (24) Reed, P.; Bhatnagar, D.; Dhar, H.; Winocour, P. H. Precise measurement of glycated serum albumin by column affinity chromatography and immunoturbidimetry. *Clin. Chim. Acta* **1986**, *161*, 191–199.
- (25) Silver, A. C.; Lamb, E.; Cattell, W. R.; Dawney, A. B. S. J. Investigation and validation of the affinity chromatography method for measuring glycated albumin in serum and urine. *Clin. Chim. Acta* **1991**, *202*, 11–22.
- (26) Kobayashi, K.; Yoshimoto, K.; Hirauchi, K.; Uchida, K. Determination of glycated proteins in biological samples based on colorimetry of 2-keto-glucose released with hydrazine. *Biol. Pharm. Bull.* **1994**, *17*, 365–369.
- (27) Dingari, N. C.; Horowitz, G. L.; Kang, J. W.; Dasari, R. R.; Barman, I. Raman spectroscopy provides a powerful diagnostic tool for accurate determination of albumin glycation. *PLoS One* **2012**, *7*, No. e32406.
- (28) Ikeda, K.; Sakamoto, Y.; Kawasaki, Y.; Miyake, T.; Tanaka, K.; Urata, T.; Katayama, Y.; Ueda, S.; Horiuchi, S. Determination of glycated albumin by enzyme-linked boronate immunoassay (ELBIA). *Clin. Chem.* **1998**, *44*, 256–263.
- (29) Choi, H.; Son, S. E.; Hur, W.; Tran, V.-K.; Lee, H. B.; Park, Y.; Han, D. K.; Seong, G. H. Electrochemical immunoassay for determination of glycated albumin using nanozymes. *Sci. Rep.* **2020**, *10*, 9513.
- (30) Kumar, D.; Bhattacharyya, R.; Banerjee, D. Pseudosterase activity-based specific detection of human serum albumin on gel. *Talanta* **2021**, *224*, No. 121906.
- (31) Chawjiraphan, W.; Apiwat, C.; Segkhoonthod, K.; Treerattrakoon, K.; Pinpradup, P.; Sathirapongsasuti, N.; Pongprayoon, P.; Luksirikul, P.; Isarankura-Na-Ayudhya, P.; Japrun, D. Sensitive detection of albuminuria by graphene oxide-mediated fluorescence quenching aptasensor. *Spectrochim. Acta. Part A, Spectrochim. Acta A Mol. Biomol.* **2020**, *231*, No. 118128.
- (32) Chawjiraphan, W.; Apiwat, C.; Segkhoonthod, K.; Treerattrakoon, K.; Pinpradup, P.; Sathirapongsasuti, N.; Pongprayoon, P.; Luksirikul, P.; Isarankura-Na-Ayudhya, P.; Japrun, D. Albuminuria detection using graphene oxide-mediated fluorescence quenching aptasensor. *MethodsX* **2020**, *7*, No. 101114.
- (33) Apiwat, C.; Luksirikul, P.; Kankla, P.; Pongprayoon, P.; Treerattrakoon, K.; Paiboonsukwong, K.; Fucharoen, S.; Dharakul, T.; Japrun, D. Graphene based aptasensor for glycated albumin in diabetes mellitus diagnosis and monitoring. *Biosens. Bioelectron.* **2016**, *82*, 140–145.
- (34) Sasar, M.; Farzadfar, A.; Abdi, Y.; Habibi-Rezaei, M. Detection of Glycated Albumin Using a Novel Field Effect Aptasensor. *IEEE Sens. J.* **2020**, *20*, 10387–10392.
- (35) Kumar, D.; Bhattacharyya, R.; Banerjee, D. Fluorimetric method for specific detection of human serum albumin in urine using its pseudoesterase property. *Anal. Biochem.* **2021**, *633*, No. 114402.
- (36) Pena-Bahamonde, J.; Nguyen, H. N.; Fanourakis, S. K.; Rodrigues, D. F. Recent advances in graphene-based biosensor technology with applications in life sciences. *J. Nanobiotechnol.* **2018**, *16*, 75.
- (37) Zor, E.; Hatay Patir, I.; Bingol, H.; Ersoz, M. An electrochemical biosensor based on human serum albumin/graphene oxide/3-aminopropyltriethoxysilane modified ITO electrode for the enantioselective discrimination of D- and L-tryptophan. *Biosens. Bioelectron.* **2013**, *42*, 321–325.
- (38) Xu, X.; Huang, J.; Li, J.; Yan, J.; Qin, J.; Li, Z. A graphene oxide-based AIE biosensor with high selectivity toward bovine serum albumin. *Chem. Commun.* **2011**, *47*, 12385–12387.
- (39) Wang, Q.-L.; Cui, H.-F.; Li, C.-L.; Song, X.; Lv, Q.-Y.; Li, Z.-Y. A multimode aptasensor based on hollow gold nanoparticles and structure switching of aptamer: fast and sensitive detection of carcinoembryonic antigen. *Sens. Actuator. A Phys.* **2020**, *2*, No. 100021.
- (40) Aye, N. N. S.; Maraming, P.; Tavichakorntrakool, R.; Chaibunruang, A.; Boonsiri, P.; Daduang, S.; Teawtrakul, N.; Prasongdee, P.; Amornkitbamrung, V.; Daduang, J. A simple graphene functionalized electrochemical aptasensor for the sensitive and selective detection of glycated albumin. *Appl. Sci.* **2021**, *11*, 10315.
- (41) Ghosh, S.; Datta, D.; Cheema, M.; Dutta, M.; Stroschio, M. A. Aptasensor based optical detection of glycated albumin for diabetes mellitus diagnosis. *Nanotechnology* **2017**, *28*, 435505.
- (42) Tabish, T.; Zhang, S. *Graphene quantum dots: syntheses, properties, and biological applications*. 2016.
- (43) Chung, S.; Revia, R. A.; Zhang, M. Q. Graphene quantum dots and their Applications in bioimaging, biosensing, and therapy. *Adv. Mater.* **2021**, *33*, No. 1904362.
- (44) Bressi, V.; Ferlazzo, A.; Iannazzo, D.; Espro, C. Graphene quantum dots by eco-friendly green synthesis for electrochemical sensing: recent advances and future perspectives. *Nanomaterials (Basel)* **2021**, *11*, 1120.
- (45) Henna, T. K.; Pramod, K. Graphene quantum dots redefine nanobiomedicine. *Mater. Sci. Eng. C Mater. Biol. Appl.* **2020**, *110*, No. 110651.
- (46) Zhang, C.; Miao, P.; Sun, M.; Yan, M.; Liu, H. Progress in miRNA detection using graphene material-based biosensors. *Small* **2019**, *15*, No. e1901867.
- (47) Zhang, H.; Wang, Y.; Zhao, D.; Zeng, D.; Xia, J.; Aldalbahi, A.; Wang, C.; San, L.; Fan, C.; Zuo, X.; Mi, X. Universal fluorescence biosensor platform based on graphene quantum dots and pyrene-functionalized molecular beacons for detection of microRNAs. *ACS Appl. Mater. Interfaces* **2015**, *7*, 16152–16156.
- (48) Mansuriya, B.; Altintas, Z. Applications of graphene quantum dots in biomedical sensors. *Sensors (Basel)* **2020**, *20*, 1072.
- (49) Singh, R. D.; Shandilya, R.; Bhargava, A.; Kumar, R.; Tiwari, R.; Chaudhury, K.; Srivastava, R. K.; Goryacheva, I. Y.; Mishra, P. K. Quantum dot based nano-biosensors for detection of circulating cell free miRNAs in lung carcinogenesis: From biology to clinical translation. *Front. Genet.* **2018**, *9*, 616.
- (50) Sittiwanichai, S.; Japrun, D.; Pongprayoon, P. The binding of apo and glucose-bound human serum albumins to a free graphene sheet in aqueous environment: Simulation studies. *J. Mol. Graphics Modell.* **2022**, *110*, No. 108073.
- (51) Bunyarataphan, S.; Dharakul, T.; Fucharoen, S.; Paiboonsukwong, K.; Japrun, D. Glycated Albumin Measurement Using an Electrochemical Aptasensor for Screening and Monitoring of Diabetes Mellitus. *Electroanalysis* **2019**, *31*, 2254–2261.
- (52) Waiwinya, W.; Putnin, T.; Pimalai, D.; Chawjiraphan, W.; Sathirapongsasuti, N.; Japrun, D. Immobilization-free electrochemical sensor coupled with a graphene-oxide-based aptasensor for glycated albumin detection. *Biosensors* **2021**, *11*, 85.
- (53) Kim, D.; Yoo, S. Aptamer-conjugated quantum dot optical biosensors: Strategies and applications. *Chemosensors* **2021**, *9*, 318.
- (54) Rohovec, J.; Maschmeyer, T.; Aime, S.; Peters, J. A. The structure of the sugar residue in glycated human serum albumin and its molecular recognition by Phenylboronate. *Chem. – Eur. J.* **2003**, *9*, 2193–2199.
- (55) Shaklai, N.; Garlick, R. L.; Bunn, H. F. Nonenzymatic glycosylation of human serum albumin alters its conformation and function. *J. Biol. Chem.* **1984**, *259*, 3812–3817.
- (56) Thornalley, P. J.; Langborg, A.; Minhas, H. S. Formation of glyoxal, methylglyoxal and 3-deoxyglucosone in the glycation of proteins by glucose. *Biochem. J.* **1999**, *344*, 109–116.

- (57) Wang, Y.; Yu, H.; Shi, X.; Luo, Z.; Lin, D.; Huang, M. Structural mechanism of ring-opening reaction of glucose by human serum albumin. *J. Biol. Chem.* **2013**, *288*, 15980–15987.
- (58) Kragh-Hansen, U. Possible mechanisms by which enzymatic degradation of human serum albumin can lead to bioactive peptides and biomarkers. *Front. Mol. Biosci.* **2018**, *5*, 63.
- (59) Kuntip, N.; Japrun, D.; Pongprayoon, P. How human serum albumin-selective DNA aptamer binds to bovine and canine serum albumins. *Biopolymers* **2021**, *112*, No. e23421.
- (60) Kenanova, V. E.; Olafsen, T.; Salazar, F. B.; Williams, L. E.; Knowles, S.; Wu, A. M. Tuning the serum persistence of human serum albumin domain III: diabody fusion proteins. *Protein Eng., Des. Sel.* **2010**, *23*, 789–798.
- (61) Schmidt, M. M.; Townson, S. A.; Andreucci, A. J.; King, B. M.; Schirmer, E. B.; Murillo, A. J.; Dombrowski, C.; Tisdale, A. W.; Lowden, P. A.; Masci, A. L.; Kovalchin, J. T.; Erbe, D. V.; Wittrup, K. D.; Furfine, E. S.; Barnes, T. M. Crystal structure of an HSA/FcRn complex reveals recycling by competitive mimicry of HSA ligands at a pH-dependent hydrophobic interface. *Structure* **2013**, *21*, 1966–1978.
- (62) Botti, V.; Marrone, S.; Cannistraro, S.; Bizzarri, A. R. Interaction between miR4749 and human serum albumin as revealed by fluorescence, FRET, atomic force spectroscopy and computational modelling. *Int. J. Mol. Sci.* **2022**, *23*, 1291.
- (63) Awang, T.; Wiriyatanakorn, N.; Saparpakorn, P.; Japrun, D.; Prapasiri, P. Understanding the effects of two bound glucose in Sudlow site I on structure and function of human serum albumin: theoretical studies. *J. Biomol. Struct. Dyn.* **2017**, *35*, 781–790.
- (64) Pongprayoon, P.; Gleeson, M. P. Probing the binding site characteristics of HSA: a combined molecular dynamics and cheminformatics investigation. *J. Mol. Graphics Modell.* **2014**, *54*, 164–173.
- (65) Humphrey, W.; Dalke, A.; Schulten, K. VMD: Visual Molecular Dynamics. *J. Mol. Graph.* **1996**, *14*, 33–38.
- (66) Robertson, M. J.; Tirado-Rives, J.; Jorgensen, W. L. Improved peptide and protein torsional energetics with the OPLSAA force field. *J. Chem. Theory Comput.* **2015**, *11*, 3499–3509.
- (67) Awang, T.; Thangsan, P.; Luksirikul, P.; Japrun, D.; Pongprayoon, P. The adsorption of glycosylated human serum albumin-selective aptamer onto a graphene sheet: simulation studies. *Mol. Simul.* **2019**, *45*, 841–848.
- (68) Jorgensen, W. L.; Chandrasekhar, J.; Madura, J. D.; Impey, R. W.; Klein, M. L. Comparison of simple potential functions for simulating liquid water. *J. Chem. Phys.* **1983**, *79*, 926–935.
- (69) Lindorff-Larsen, K.; Piana, S.; Palmo, K.; Maragakis, P.; Klepeis, J. L.; Dror, R. O.; Shaw, D. E. Improved Side-Chain Torsion Potentials for the Amber FF99SB protein force field. *Proteins* **2010**, *78*, 1950–1958.
- (70) Darden, T.; York, D.; Pedersen, L. Particle mesh Ewald: An N-log(N) method for Ewald sums in large systems. *J. Chem. Phys.* **1993**, *98*, 10089–10092.
- (71) Hess, B.; Bekker, H.; Berendsen, H. J. C.; Fraaije, J. G. E. M. LINCS: a linear constraint solver for molecular simulations. *J. Comput. Chem.* **1997**, *18*, 1463–1472.
- (72) Bussi, G.; Donadio, D.; Parrinello, M. Canonical sampling through velocity rescaling. *J. Chem. Phys.* **2007**, *126*, No. 014101.
- (73) Panman, W.; Japrun, D.; Pongprayoon, P. Exploring the interactions of a DNA aptamer with human serum albumins: simulation studies. *J. Biomol. Struct. Dyn.* **2017**, *35*, 2328–2336.
- (74) Ketrat, S.; Japrun, D.; Pongprayoon, P. Exploring how structural and dynamic properties of bovine and canine serum albumins differ from human serum albumin. *J. Mol. Graphics Modell.* **2020**, *98*, No. 107601.
- (75) Vilhena, J. G.; Rubio-Pereda, P.; Velloso, P.; Serena, P. A.; Perez, R. Albumin (BSA) adsorption over graphene in aqueous environment: influence of orientation, adsorption protocol, and solvent treatment. *Langmuir* **2016**, *32*, 1742–1755.
- (76) Huang, S.; Qiu, H.; Lu, S.; Zhu, F.; Xiao, Q. Study on the molecular interaction of graphene quantum dots with human serum albumin: combined spectroscopic and electrochemical approaches. *J. Hazard. Mater.* **2015**, *285*, 18–26.